ARCHITECTURE CIVIL ENGINEERING ENVIRONMENT
The Silesian University of Technology No. 2/2009

MWW3 MODEL FOR CONCRETE – ADJUSTMENT OF FAILURE AND YIELD SURFACES FOR USE IN COMPUTATIONAL FEM SYSTEM MAFEM3D

Stanisław MAJEWSKI [a], Grzegorz WANDZIK [b]

[a] Professor, Faculty of Civil Engineering, The Silesian University of Technology, Akademicka 5, 44-100 Gliwice, Poland
E-mail address: *Stanislaw.Majewski@polsl.pl*

[b] Dr., Faculty of Civil Engineering, The Silesian University of Technology, Akademicka 5, 44-100 Gliwice, Poland
E-mail address: *Grzegorz.Wandzik@polsl.pl*

Received: 04.02.2009; Revised: 20.03.2009; Accepted: 05.04.2009

Abstract

Definitions of the failure surface, as well as evolution of yield surface are crucial elements in nonlinear FEM analysis of reinforced concrete members and structures carried out with use of elasto-plastic material model. Procedure of formation of these surfaces in *MWW3* material model used in author's computational system *Mafem3D* has been described.
In *MWW3* model, each meridian section of yield section is composed of straight-linear segment in the middle part and two caps: parabolic from the side of mean tensile stresses and circular from the side of compressive stresses.

Formation of the linear segments of tensile and compressive meridians is a result of approximation of laboratory experiments performed in the complex stress states. Caps definition is based on the meridians course adjustment to the basic strength properties and assuring basic requirements of the surfaces shape such as: continuity, smoothness and convexity. Procedure used for equations definition, necessary for their adjustment with laboratory tests results and possibility of their implementation in numerical algorithm used in computational system has been described.

Streszczenie

W nieliniowej analizie MES elementów i konstrukcji żelbetowych prowadzonej z wykorzystaniem sprężysto-plastycznego modelu materiałowego betonu bardzo istotną rolę pełni sposób zdefiniowania powierzchni granicznej oraz ewolucja powierzchni plastyczności. W artykule przedstawiono sposób kształtowania tych powierzchni w modelu *MWW3* stosowanym w autorskim systemie komputerowym *Mafem3D*.
W opisywanym modelu, dowolny przekrój południkowy przez powierzchnię plastyczności składa się z odcinka prostego w środkowej części oraz dwóch nasadek: parabolicznej po stronie średnich naprężeń rozciągających oraz kołowej po stronie średnich naprężeń ściskających.
Ukształtowanie prostoliniowych odcinków południków ściskania i rozciągania wynika z przybliżenia wyników badań doświadczalnych prowadzonych w złożonych stanach naprężenia. Zdefiniowanie nasadek bazuje na dostosowaniu przebiegu południków do wartości podstawowych cech wytrzymałościowych betonu oraz zapewnienia podstawowych wymagań stawianych powierzchniom, takich jak ciągłość, gładkość oraz wypukłość. W artykule opisano sposób definiowania równań zapewniających powierzchniom zgodność z wynikami podstawowych badań wytrzymałościowych oraz możliwość ich dostosowania do algorytmu numerycznego wykorzystywanego w programie komputerowym.

Keywords: **Concrete; Elasto-plastic material model; Failure and yield surfaces; Nonlinear FEM analysis; Complex stress state.**

1. INTRODUCTION

In the era of computational analysis of reinforced concrete structures there is a great number of sophisticated material models for concrete. On the other hand, in design practise static calculations are predominantly carried out with the use of the simplest linear-elastic model and only some major drawbacks are corrected at the stage of sizing. Gap between those approaches is huge.

There is a long list of technical problems, where excessive simplicity of linear-elastic material model for concrete can not be accepted, while too sophisticated models are not possible to apply, because of difficulty in the model parameters identification. Use of developed models is still difficult in all cases where relatively large problems must be solved. There is still free space for simple elasto-plastic models for concrete. Incorporation of such models into computational systems leads to refinement of results. Dozens of real structural problems, including 3D tasks can be much more realistically analysed in terms of elasto-plasticity. Relatively simple definition of material parameters on the basis of the laboratory tests is a strong advantage of this approach.

For more than last 15 years, authors have worked on nonlinear FEM computer system called *Mafem* [1]. It is focused on problems concerning calculations of concrete [2,3,4] and masonry [5] structures, including problems of interaction between structure and subsoil [6]. At the beginning it was used for 2D problems, while later it was extended on 3D tasks. Generally, program is designed for calculations of macro scale problems with consideration of 3D stress and strain states. This paper is dedicated to failure and yield surfaces creation and their mathematical description, that are implemented in this software. Compliance with basic laboratory experiments and solidity of equations to fulfil requirements of numerical analysis is necessary. The way in which it is achieved is described below.

2. GENERAL DESCRIPTION OF MATERIAL MODEL FOR CONCRETE

Material model for concrete currently used in *Mafem3D* computational system called *MWW3* is a modification of *Willam* and *Warnke* concept [7]. This model could be classified to the group of continuum models. It is a modification of previous solutions, after removing some drawbacks and in fact widening the domain of its use and improving the accuracy of calculations. Described model belongs to the group of elasto-plastic material models with isotropic softening. The model is designed for 3D problems, thus all formulas are defined in 3D stress and strain states.

To achieve simplicity of concrete description some assumptions have been made. Until cracking or crashing occurs, concrete is treated as homogeneous and isotropic material. These properties are valid till failure surface is reached by the stress path. In *MWW3* model smeared crack representation is assumed. In reinforced concrete members steel and concrete are modelled independently. Reinforcing steel bars are represented by the linear elements joint to the nodes of FEM structure. Both simplifications are acceptable in large scale problems for which this model is dedicated.

In calculations carried out with the use of *Mafem3D* loads are treated as immediate. Behaviour of concrete does not include simulation of time-dependent phenomena such as creeping or shrinkage.

Definition of material model consists of the following components:

- failure criterion specified in the term of the failure/boundary surface defined in the stress space,
- hardening and softening rules describing evolution of the yield surface,
- stress – strain relations in the elastic region,
- flow rule determining deformability control of material in the post-elastic phase of work.

In this paper, first two components have been widely described.

Process of model creation requires definition of functions used later in the program code. Numbers specified as a data set must finally define realistic behaviour of concrete. In practice, it is quite important to have possibility of parameters identifications. It is usually expected to specify shape of the failure surface, softening rule, behaviour in elastic and post-elastic phase with the use of basic material parameters.

In computational systems, description of material behaviour should be sufficiently precise and relatively simple. Simplicity of derived relations helps to decrease numerical effort needed at the stage of calculations and keep better control on it. It is needed to incorporate model, which is general and possibly strict for arbitrary loading paths. Possibility of creation of complete mathematical description on the basis of laboratory tests does not exist, so such a description is always combined as a mixture of experimental data and theoretical prediction.

Relations for the concrete are specified in the stress space defined by mean normal stress σ_m octahedral shear τ_{oct} and Lode's angle Θ. Uniaxial compressive strength of concrete f_c is treated as a basic parameter. Many formulas used for model description are written with the use of normalised (sometimes called equivalent) and unitless variables s_m and t_0, representing stresses σ_m and τ_{oct} with respect to uniaxial compressive strength f_c:

$$t_0 = \frac{\tau_{oct}}{f_c} \quad \text{and} \quad s_m = \frac{\sigma_{oct}}{f_c} \tag{1}$$

Variable t_0 describing location of tensile meridian is denoted with superscript "t", while compressive meridian is denoted with a superscript "c". Variables expressing basic strength properties of concrete, such as uniaxial tensile strength ft or biaxial compressive strength f_{cc} are also substituted by unitless parameters m_t and m_{cc}. These parameters, describing ratio of appropriate strength to the uniaxial compressive strength f_c are defined as follows:

$$m_t = \frac{f_t}{f_c}; \quad m_{cc} = \frac{f_{cc}}{f_c} \tag{2}$$

The same notation is used in graphs presented in the paper, showing failure and yield surfaces usually drawn in normalised coordinates s_m and t_o.

3. FAILURE SURFACE

Failure surface expressing failure criterion is one of the crucial elements in material modelling. Alternatively, failure surface is also named as a boundary surface. Location of this surface defines generalised strength of concrete in complex stress state and splits stress space into two regions of possible and unreal states. It also determines different stages of the material's behaviour before and after destruction. For concrete it is definitely equivalent to a loss of isotropy. Behaviour of concrete is complicated, thus the failure criterion cannot be defined just on the basis of a simple theoretical assumption. A realistic approach must take into account a wide range of laboratory tests, including two and three dimensional states of stress. The reliability of tests carried out by *Balmer* [8], *Kupfer* [9], *Richart et al.* [10], *Mills & Zimmerman* [11] are widely accepted. These experiments results supplemented with the results of uniaxial compression and tension tests create the base for determination of the failure criterion for concrete.

There are many concepts of failure surface formation. In general, its shape is known, but there is long list of various approximations. They are always based on the tests made in laboratory conditions. View of typical failure surface is presented in figure 1.

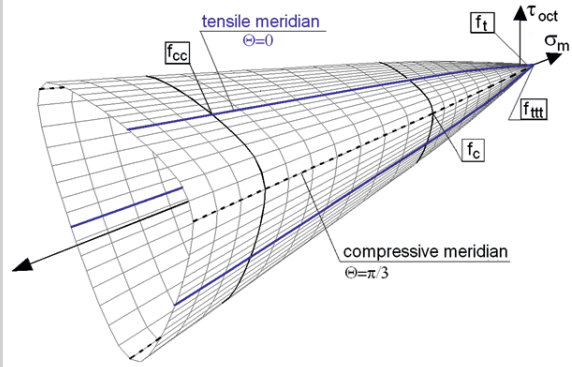

Figure 1.
3D view of the shape of the failure surface for concrete

Definition of boundary surface shape approximated by *Willam* and *Warnke* [7] with the use of second order polynomial (3) is widely accepted.

$$t_o = a_2 s_m^2 + a_1 s_m + a_0, \tag{3}$$

General concept of *Willam* and *Warnke* boundary surface was adopted in *MWW3* model. In 3 parameter *Willam-Warnke* model, tensile meridian is directly coming through points representing uniaxial tensile strength and biaxial compressive strength. It crosses mean stress axis at the point representing triaxial tensile strength, expressed in normalised coordinates by $(0,m_{ttt})$ value. Compressive meridian is coming through the same point on the mean stress axis and through the point representing uniaxial compressive strength of concrete. Such a definition assures good approximation of test results for the mean compressive stresses region not exceeding $\sigma_m = -1.5f_c$. For higher compressive stresses the convergence is much worse.

In *MWW3* model for concrete shape of *Willam-Warnke* boundary surface was slightly refined to obtain better approximation to tests results up to the stress level equal to $\sigma_m = -5f_c$. Both meridians (tensile and compressive) are composed of three parts: straight-linear in the middle and two caps closing surface from both compressive and tensile sides. Linear segments of meridians are expressed in the general form as:

- tensile meridian: $t_o^t = c_{1t} s_m + c_{0t}$, (4)
- compressive meri $t_o^c = c_{1c} s_m + c_{0c}$, (5)

Despite the *Willam-Warnke* proposition, in *MWW3* model straight-linear part of tensile meridian is constructed in such a shape to come through the point representing biaxial compressive strength of concrete. Slope of this line (c_{1t}) is determined to achieve

the best approximation of the laboratory tests carried out in complex stress states (where Lode's angle $\Theta = 0°C$ corresponds to the tensile meridian). Equation of the straight linear segment of tensile meridian determined with the use of least square method is as follows:

$$t_o^t = -0.470 s_m + 0.185 \tag{6}$$

Analysis of tests results leads to the conclusion that straight linear approximation of results in the region close to the point representing uniaxial tensile strength is not strict enough. Line in the form (6) intersects the mean stress axis at point s_m = 0.393. Nonlinear approximation of meridians in zone of mean tensile stresses is described later on.

Definition of the linear part of compressive meridian is determined with the use of two boundary conditions. First, it was assumed that compressive meridian should cross mean stress axis at the same point at which the tensile meridian does. In the same way as for tensile meridian, slope of the compressive meridian (c_{1c}) is determined with the use of least square method. In fact, coefficients of both lines have been determined in the same step after normalisation of laboratory results for tensile and compressive meridians. Equation of straight linear part of the compressive meridian in the slope intercept form is as follows:

$$t_o^c = -0.713 s_m + 0.280 \tag{7}$$

Traces of both meridians related to the experimental results are shown in figure 2.

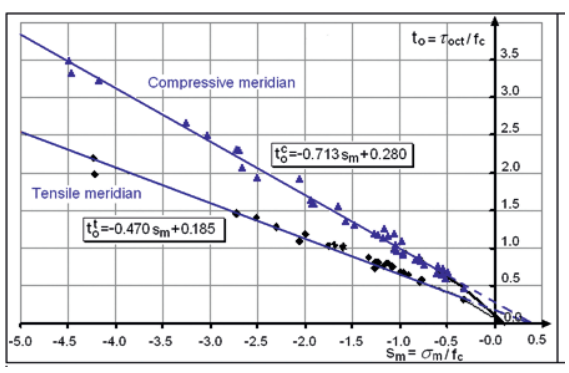

Figure 2.
Traces of linear approximation of meridians related to experimental results

The tensile and compressive meridians of the *MWW3* failure surface as well as the triaxial and uniaxial test results [8,9,12,13] together with those carried on at the Silesian University of Technology are presented in figure 2. The straight-linear meridians given by (6) and (7) correspond very well with triaxial compression test results for $-5.0 < s_m \leq -2m_{cc}/3$. Outside this region the closing cap (tension cut-off) must be determined (fig. 3). Second order polynomial is used for description of the cap from the side of tension. To obtain the smooth failure surface, it is required that both parabolic meridians must be tangentially joint to the corresponding meridians of the main, conical part of the surface.

Equations of the tensile and compressive meridians of the closing cap from the tension side of the failure surface are assumed in the following general form:

$$t_{o,n}^t = a_{2t} s_m^2 + a_{1t} s_m + a_{0t}, \quad t_{o,n}^c = a_{2c} s_m^2 + a_{1c} s_m + a_{0c} \tag{8}$$

Shape of these parabolic parts of meridians is shown in figure 3.

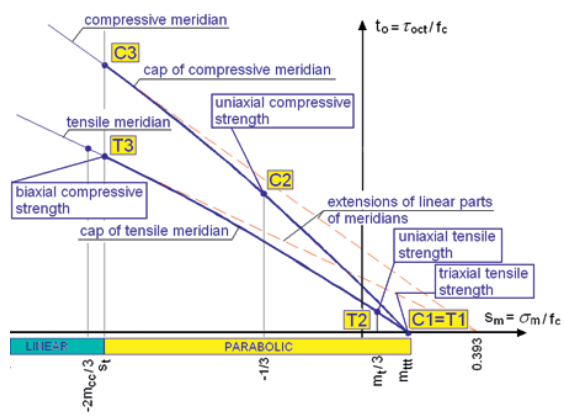

Figure 3.
Tensile and compressive meridians of the cap from the side of tension

To define parabolic parts of meridians, six coefficients in quadratic equations (8) as well as fictitious triaxial tensile strength m_{ttt} and mean stress coordinate of the contact point s_t must be determined. They are obtained on the basis of the stress coordinates of total number of 6 points lying on the curved parts of the meridians. Points denoted with symbols *T1..T3* are situated on the tensile meridian, while these denoted with symbols *C1..C3* are situated on the compressive meridians. System of the following eight equations (9) – (16) is used for finding all eight constants mentioned above:

points on tensile meridian:

point *T1*: apex of the boundary surface – triaxial ten-

sile strength of concrete ($s_m = m_{ttt}$; $t_o = 0$):

$$t_{ok}^t = a_{2t} m_{ttt}^2 + a_{1t} m_{ttt} + a_{0t} = 0 \tag{9}$$

point *T2*: uniaxial tensile strength of concrete ($s_m = m_t/3$; $t_o = m_t\sqrt{2}/3$):

$$t_{ok}^t = a_{2t}(m_t/3)^2 + a_{1t}\, m_t/3 + a_{0t} = m_t\sqrt{2}/3 \tag{10}$$

point *T3*: contiguity point between linear and curved parts of tensile meridian ($s_m = s_t$; $t_o = c_{1t}s_t + c_{0t}$):

$$t_{ok}^t = a_{2t} s_t^2 + a_{1t} s_t + a_{0t} = c_{1t} s_t + c_{0t} \tag{11}$$

point *T3*: smoothness of the tensile meridian at the contiguity point ($s_m = s_t$; $t_o = c_{1t}s_t + c_{0t}$):

$$\left(t_{ok}^t\right)' = 2a_{2t} s_t + a_{1t} = c_{1t} \tag{12}$$

points on the compressive meridian:

point *C1*: apex of the boundary surface – triaxial tensile strength of concrete ($s_m = m_{ttt}$; $t_o = 0$):

$$t_{ok}^c = a_{2c} m_{ttt}^2 + a_{1c} m_{ttt} + a_{0c} = 0 \tag{13}$$

point *C2*: uniaxial compressive strength of concrete ($s_m = -1/3$; $t_o = \sqrt{2}/3$):

$$t_{ok}^c = a_{2c}/9 - a_{1c}/3 + a_{0c} = \sqrt{2}/3 \tag{14}$$

point *C3*: contiguity point between linear and curved parts of compressive meridian ($s_m = s_t$; $t_o = c_{1t}s_t + c_{0t}$):

$$t_{ok}^c = a_{2c} s_t^2 + a_{1c} s_t + a_{0c} = c_{1c} s_t + c_{0c} \tag{15}$$

point *C3*: smoothness of the compressive meridian at the contiguity point ($s_m = s_t$; $t_o = c_{1t}s_t + c_{0t}$):

$$\left(t_{ok}^c\right)' = 2a_{2c} s_t + a_{1c} = c_{1c} \tag{16}$$

Solving system of 8 equations (9)–(16) determination of 6 unknown coefficients in parabolas (8), as well as the coordinates of the theoretical triaxial tensile strength m_{ttt} and contact point st of curvilinear cap meridians with straight-line meridians of the main part of the surface is enabled. All these values are determined as a function of uniaxial tensile strength (precisely as a function of m_t multiplier: $m_t = f_t / f_c$). The calculations carried out for $0.05 \le m_t \le 0.15$ gave the following formulas:

$$\begin{aligned}
m_{ttt} &= 2.210 m_t^2 + 0.695 m_t \\
s_t &= -15.135 m_t^2 + 0.544 m_t - 0.608 \\
a_{2t} &= -7.748 m_t^2 + 4.284 m_t - 0.575 \\
a_{1t} &= -4.878 m_t^2 + 3.814 m_t - 1.119 \\
a_{0t} &= -0.908 m_t^2 + 0.828 m_t \\
a_{2c} &= -11.756 m_t^2 + 6.500 m_t - 0.873 \\
a_{1c} &= -7.402 m_t^2 + 5.788 m_t - 1.698 \\
a_{0c} &= -1.377 m_t^2 + 1.256 m_t
\end{aligned} \tag{17}$$

In such defined caps of failure surface, uniaxial tensile strength of concrete plays very important role, because it influences all 8 coefficients. In *Mafem3D* system, one of the input parameter is a uniaxial tensile strength of concrete f_t. In practical cases, where tensile strength of concrete can not be measured, it is suggested t_o assume its value on the formulas referring to the uniaxial tensile strength obtained as a function of uniaxial compressive strength. The most popular relations used for that purpose are based on the *Feret* equation:

$$f_t = \beta \cdot f_c^{2/3} \tag{18}$$

Coefficient β modelling relation (18) is not unambiguous. Efficiency of this formula is not perfect, but there are many reasons having influence on it. Among them, there is big sensitivity of tests for tensile strength to the external conditions (i.e. all inaccuracies occurring) as well as sample shape and size. Because of the high dispersion of results, strict correlation between both strengths is not possible to established. It is accepted that coefficient β should be assumed as a value within the range from 0.3 to 0.5 [14] (although other resources indicate even wider range of β coefficient: 0.4 to 0.8 [15]). In design based on the *Eurocode* standards [16], conservative value of the coefficient β =0.3 is assumed. In design, there is also a hidden influence of safety factors included, because it is recommended to estimate mean value of tensile strength with regard to characteristic value of compressive strength. In the literature, information about the influence of the aggregate type on this correlation could be also found. According to the test results [17] it is recommended to assume values of coefficient β within the range 0.5÷0.6.

Referring to the scatter of tensile strength it is suggested to assume values a little bit smaller (more often if some safety margin should be involved in calculation). Example of the influence of the uniaxial compressive strength f_c and β coefficient on the parameter m_t and coefficients of parabolas equations describing cap of the failure surface is illustrated by the numbers collected in the table 1.

Table 1.
Coefficients used in formulas describing caps of tensile and compressive meridians with regard to compressive strength and β coefficients

input data				
f_c [MPa]	30	30	50	50
β	0.3	0.5	0.3	0.5
f_t [MPa]	2.90	4.83	4.07	6.79
m_t	0.097	0.161	0.081	0.136
additional parameters				
m_{ttt}	0.088	0.169	0.071	0.135
s_t	-0.697	-0.912	-0.664	-0.813
cap of tensile meridian				
a_{2t}	-0.234	-0.086	-0.278	-0.137
a_{1t}	-0.796	-0.631	-0.841	-0.691
a_{0t}	0.071	0.110	0.061	0.096
cap of compressive meridian				
a_{2c}	-0.355	-0.131	-0.421	-0.207
a_{1c}	-1.208	-0.958	-1.275	-1.048
a_{0c}	0.108	0.166	0.093	0.145

Traces of two pairs of boundary surfaces meridians caps obtained for the concrete differs with uniaxial tensile strengths are shown in figure 4. Both types of concrete for which meridians are drawn in figure 4 have the same compressive strength f_c = 30 MPa (both compressive meridians intersect for the s_m= -1/3 in point *C2*), while β coefficient is equal 0.3 for the surfaces drawn with a red colour and 0.5 for those drawn with a blue one. To achieve necessary smoothness of the surfaces, tangential points *C3* and *T3* (the same for both meridians) are moved toward higher compressive stresses. In case of higher tensile strength, tangential points are situated closer to the vertical line representing equivalent mean stress equal to $2m_{cc}/3$.

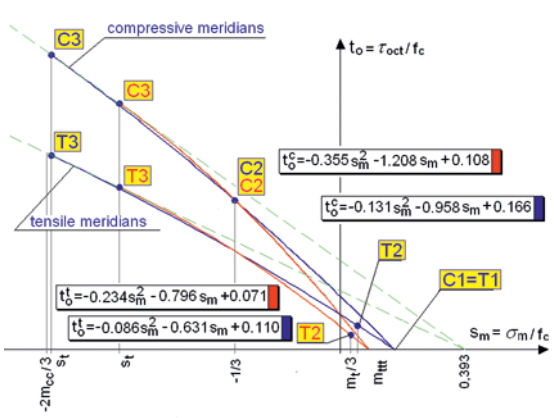

Figure 4.
Shape of caps of tensile and compressive meridians on the tensile mean stress side

Coefficients in equations of all other meridians of the failure surface (for all arbitrary Lode's angles within the range 0°C < Θ < 60°C) can be calculated according to the assumed shape of the deviatoric section of the surface. In *MWW3* model, Willam-Warnke's elliptical approximation (fig. 5) is adopted. An unquestionable advantage of this three elliptical section is its smoothness and convexity, though it probably gives a little bit overestimated value for the shear strength of concrete. In mathematical description used in the computer application, relative (non-dimension value) radius $\rho_{(\Theta)}$ is used. It expresses radius of the surface (distance measured to its meridians at any Lode's angle) with regard to the radius of the compressive meridian at the same deviatoric section $\rho_{(\Theta)} = r_\Theta / r_c$ (fig. 5). The following relation is used for that purpose:

$$\rho_{(\Theta)} = \frac{2\left(1-\rho^2\right)\cos\Theta + (2\rho-1)\sqrt{4\left(1-\rho^2\right)\cos^2\Theta + 5\rho^2 - 4\rho}}{4\left(1-\rho^2\right)\cos^2\Theta + (1-2\rho)^2} \quad (19)$$

The coefficient ρ in (19) is equal to the lowest value of $\rho_{(\Theta)}$, equal to the ratio of tensile to compressive radii in the deviatoric section of the failure surface.

In the *MWW3* model, which is similar to the *Willam-Warnke* 3 parameter model, this ρ coefficient is a constant (hydrostatic pressure independent value) and can be easily determined as a ratio of corresponding coefficients in formulas describing linear segments of tensile and compressive meridians (6) and (7):

$$\rho = c_{1t}/c_{1c} = -0.470/-0.713 = c_{0t}/c_{0c} = 0.184/0.280 = 0.659 \quad (20)$$

Well known elliptical approximation of deviatoric section proposed by *Willam* and *Warnke* (chosen in *Mafem3D*) is shown in figure 5.

4. YIELD SURFACE

For pressure sensitive materials associated flow rule is often unrealistic and in developed models it is usually replaced by the non-associated flow rule. Nevertheless, it must be considered that non associated plasticity results in loss of symmetry of the stiffness matrix. It also requires definition of plastic potential function. Because of the lack of reliable experimental data, defining the real behaviour at this

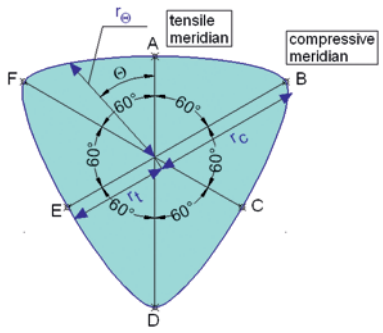

Figure 5.
Deviatoric section of the failure surface adopted from the Willam-Warnke concept [7]

stage of loading, in *MWW3* model associated flow rule have been assumed. Although, such a description is not fully adequate, but in practical computational application it considerably simplifies mathematical description and calculation process.

In *MWW3* model linearly parabolic approximation of the stress-strain relation is assumed. In the initial stage of the uniaxial loading (for $\sigma \leq$ elim f_c) we deal with the linear stress-strain relation and non-linearity appears for higher stress levels. Non-dimensional coefficient elim indicates the conventional elasticity limit. Moreover, it is assumed, that for $\sigma > e_{lim} f_c$ only plastic deformation occurs, thus the unloaded branch of stress-strain curve is parallel to the initial, linear part of this curve at the loading stage. It is quite convenient to assume e_{lim}, as a parameter determines not only elasticity limit but also the initial shape of the yield surface. In *MWW3* model, this initial position of yield surface is determined on the basis of the failure surface, treating e_{lim}. as a scale factor. Elastic domain is limited by the initial position of the yield surface. Elasticity limit is expressed in terms of the uniaxial strength f_c using the following formula:

$$e_{\lim} = 1 - \exp(-f_c/80) \tag{21}$$

After reaching yield surface concrete exhibits hardening, until load path achieves failure surface. To enable irreversible strains on stress paths running below the critical state line to be revealed, the yield surface must be closed with a cap on the compressive side (fig. 6).

Considering the isotropic hardening rule the equation of the yield surface is derived from the equation of the failure surface. Its definition, similar to the failure surface, is split into three regions: straight linear in the middle closed with caps on both ends. Shape of a deviatoric section is also retained.

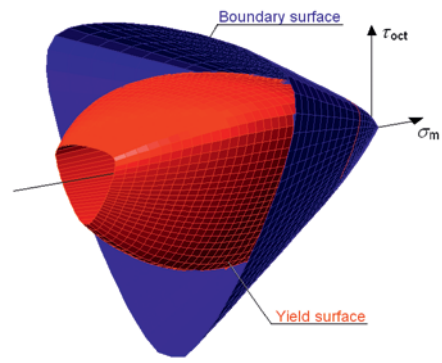

Figure 6.
3D view of the developing yield surface inside the boundary surface

At the hardening and softening stage, formulas used for description of yield surface, as a function of Lode's angle Θ are as follows:

in the range of straight linear part of meridian:

$$t_o(\Theta) = \left(c_{1t} s_m + c_{0t} y_v\right) y_i \frac{\rho_\Theta}{\rho} \tag{22}$$

in the range of the cap from the tensile side (for $s_m > s_t$):

$$t_o(\Theta) = \left(a_{2t} s_m^2 + a_{1t} s_m + a_{0t} y_v\right) y_i \frac{\rho_\Theta}{\rho} \tag{23}$$

In formulas (22) and (23) c_{1t}, c_{0t}, a_{2t}, a_{1t} and a_{0t} stand for coefficients, which define the tensile meridian segments of the boundary surface *MWW3* (6) and (17), ρ_Θ is given by (19) and ρ indicates the ratio of deviatoric section radii (20).

Evolution of the yield surface due to material hardening or softening are described by non-dimensional yield functions y_v, y_i. Yield function yv depends on the sum of increments of the plastic parts of volumetric as well as deviatoric strains, while y_i function depends only on the plastic part of the deviatoric strain.

At the stage of hardening, function yi for the complex stress state is obtained by transposition of the simple formula defined for the uniaxial stress state. For uniaxial stress state equation is as follows:

$$y_i = e_{\lim} + \left(1 - e_{\lim}\right)\sqrt{\frac{\varepsilon_{pl}}{\Delta_{pl}}\left(2 - \frac{\varepsilon_{pl}}{\Delta_{pl}}\right)} \tag{24}$$

where:

ε_{pl} – plastic strain at the current stress level,

Δ_{pl} – plastic strain at the stress level equal to the uniaxial material strength.

Obviously, at the stage of hardening yi function argument varies between $0 \le \varepsilon \le \Delta_{pl}$ and function returns values, which varies between $e_{lim} \le y_i \le 1$.

Transposition to the complex stress-state requires replacing linear strains ε_{pl} and Δ_{pl} with more general parameters appropriate in complex stress state. For deviatoric hardening/softening the plastic part of the shear octahedral strain is adopted as a parameter:

$$\kappa_2 = \frac{2}{3}\sqrt{\left(\varepsilon_{1,pl}-\varepsilon_{2,pl}\right)^2+\left(\varepsilon_{2,pl}-\varepsilon_{3,pl}\right)^2+\left(\varepsilon_{3,pl}-\varepsilon_{1,pl}\right)^2} \quad (25)$$

In the complex stress state, Δ_{pl} should represent plastic part of the shear octahedral stress at failure. Its value is not known for every possible stress-path. For the complex stress state we define parameter s_l (called stress level), corresponding to the stress-ratio level. It refers to the ratio of current octahedral shear stress with regard to the octahedral shear at the failure (for the same mean normal stress level):

$$s_l = \tau_{oct} / \tau_{oct}^f \quad (26)$$

Approximating curved branches of ascending and descending parts of uniaxial stress-strain diagram with ellipse and finding some similarities with the complex stress state following equation could be formulated:

$$\frac{\left(s_l - e_{\lim}\right)^2}{\left(1-e_{\lim}\right)^2} + \left(1-\frac{\kappa_2}{\Delta_{pl}}\right)^2 = 1 \quad (27)$$

Deriving κ_2/Δ_{pl} from the equation (27) following solution is obtained:

$$\frac{\kappa_2}{\Delta_{pl}} = 1 - \frac{\sqrt{-s_l^2 + 2e_{\lim}s_l - 2e_{\lim} + 1}}{1-e_{\lim}} \quad (28)$$

After substituting (28) to equation (24), following formula for the deviatoric hardening function yi is achieved:

$$y_i = e_{\lim} - \left|\frac{e_{\lim}-s_l}{e_{\lim}-1}\right| \cdot (e_{\lim}-1) \quad (29)$$

For the range of the octahedral stress level $e_{lim} \le sl \le 1$, for which function is used, following simplification is achieved:

$$y_i = s_l\,, \quad (30)$$

Although the hardening process depends on s_l instead of hardening parameter κ_2, the last variable must be also determined because its value corresponding with the violation of the failure surface becomes furthermore a material parameter, which is necessary during the deviatoric softening process. The plastic part of strain vector κ_2 can be easily calculated as:

$$[\varepsilon_{pl}]=[\varepsilon]\,[\mathbf{D}^e]^{-1}[\sigma], \quad (31)$$

As soon as the yield function reaches its upper limit $y_i = 1$, the loading surface (except for the cap on the compression side) coincides with the failure surface. A further increase of plastic strain results in softening and shrinking of the loading surface due to a decrease of the yield function y_i to zero.

Following the same procedure, which was applied for hardening, deviatoric softening yield function y_i could be determined with the use of exponential approximation:

$$y_i = \exp\left(-\left(\frac{\kappa_2-\Delta_{pl}}{\sqrt{2}\Delta_{2,pl}}\right)^2\right) \quad (32)$$

Function (29) is valid for $\kappa_2 \ge \Delta_{pl}$ and returns values starting from $y_i = 1$ (for $\kappa_2=\Delta_{pl}$) to $y_i = 0$. In the complex stress state, for Δ_{pl} the real value of plastic strain κ_2, corresponding with the extreme expansion of the yield surface ($y_i = 1$) is substituted. It can be convenient to express the distance ε_{cu} -ε_c on the descending part of the stress-strain diagram in terms of Δ_{pl} as ε_{cu} -ε_c =$\lambda\Delta_{pl}$=Δ_{pl}2,pl. In this case, increment dy_i of the softening function y_i is negative, what represents shrinkage of the yield surface.

Both, deviatoric hardening and softening influences the inclination angle of the straight-linear meridians of the yield surface and indirectly affects the shape of both caps (fig. 7).

The hardening or softening occurring in the region of caps depends on the plastic increment of the volumetric strain.

$$\kappa_1 = \varepsilon_{v,pl} = \varepsilon_{1,pl} + \varepsilon_{2,pl} + \varepsilon_{3,pl} \quad (33)$$

The cap in tension region is subjected only to softening due to positive increments of volumetric strains, which generate negative increments of the non-dimensional yield function y_v. Its value varies in the range $1 \ge y_v \ge 0$. The character of these changes should be determined on the basis of laboratory tests in tension. Considering the brittle character of failure in tension, the realistic determination of this branch seems to be impossible. Therefore for descending branch of σ-ε diagram the same function as in compression was adopted. Additionally it was assumed Δ_{pl}=0 and the distance between extreme and inflex-

ion point on the descending branch of stress-strain diagram expressed in terms of volumetric strain was indicated as $\Delta_{2,pl}$. Considering the brittle character of failure at tension this value should be rather assumed then determined in laboratory tests. Following these assumptions volumetric softening function has been written in the form:

$$y_v = 1 - \exp\left(-\frac{(\kappa_1 + \kappa_2)^2}{2\Delta_{2,pl}^2}\right) \tag{34}$$

The cap on the compressive side can undergo hardening at compression due to volumetric compression. We deal with hardening if the stress-path intersects the yield surface at $s_m < c_n$ (c_n is the coordinate of the centre of circular cap meridian). This corresponds with paths running below the critical line state.

Evolution of the yield surface due to various forms of hardening and softening is presented in figure 7.

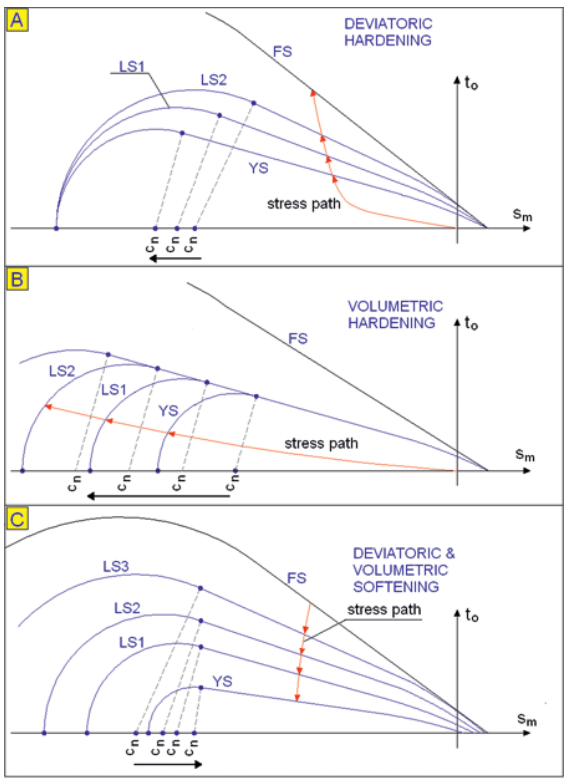

Figure 7.
Yield surface: A. deviatoric hardening, B. volumetric hardening, C. deviatoric and volumetric softening *YS* – yield surface, *LS* – loading surface, *FS* – failure/boundary surface

Initially $y_v = 1$. Positive volumetric strain (dilatation) results in softening in the region of the cap in the tensile zone. The yield coefficient changes in the range $0 \le y_v \le 1$. In the incremental algorithm value of y_v is calculated not only when dilatation occurs, but also in case of concrete damage both due to deviatoric failure and crushing under hydrostatic compression. During unloading as well as in case of a negative increment of plastic volumetric strain, the yield coefficient remains invariable. On the tensile side the softening results in moving the yield surface apex towards zero.

The second yield coefficient y_i depends on the increment of the plastic part of the deviatoric strain, which is calculated as a square root from the second deviatoric strain invariant. This invariant is always positive, though its value can increase or decrease. The new value of the yield coefficient y_i is determined only in case of increasing deviatoric plastic strain. Initially $y_i = e_{lim}$. In the hardening phase, when yield surface expands y_i increases from $y_i = e_{lim}$ to $y_i = 1.0$. If both yield functions values reach $y_v = y_i = 1.0$ the yield surface osculates with the boundary surface. From this state it can only shrink in the softening process as y_i decreases from one to zero.

Softening of concrete is exhibited by the shrinkage of yield surface. Even for high values of mean stresses σ_m, deviation from hydrostatic pressure leads to the material softening. It causes that closure of the yield surface with the cap from the side of the high compressive stresses is also required. In *MWW3* model this cap is constructed with the use of circular meridians. All these meridians are tangentially joint with appropriate straight-linear segments and have one common apex. This apex is situated at the intersection of circles with the mean stress axis at the point, whose coordinate in normalised system of octahedral stresses is expressed with the symbol m_{ccc}. In *MWW3* material model for concrete value of m_{ccc} has a status of dimensionless material parameter. It represents such a hydrostatic pressure $m_{ccc}f_c$, which is a limit of elastic volumetric strain. Always, when hydrostatic pressure exceeds this value (is more negative) plastic volumetric strain appears.

The construction of the closing circular cap on the compressive side of the yield surface is presented in figure 8. For simplification, m_{ccc} was assumed at such a level that the closing cap from the compressive side would always contact with meridians of the yield surface along the straight-linear segment of its meridians (not with the parabolic cap from the tensile side). To fulfil this requirement, for each meridian we

should get $s_c < s_t$. To assure this assumption limit m_{ccc} value could be calculated from equation:

$$m_{ccc} < \frac{\sqrt{\left(c_{1t}^2+\rho^4\right)\left(7c_{1t}-10c_{0t}\right)}-7c_{1t}^2+10c_{1t}c_{0t}-7\rho^4}{10\rho^4} \quad (35)$$

where:

c_{1t} and c_{0t} are coefficients of equation describing linear segment of the tensile meridian of failure surface,

Substituting appropriate data for the equation of *MWW3* failure surface $m_{ccc} < -3.725$ is obtained, what seems to be a realistic value.

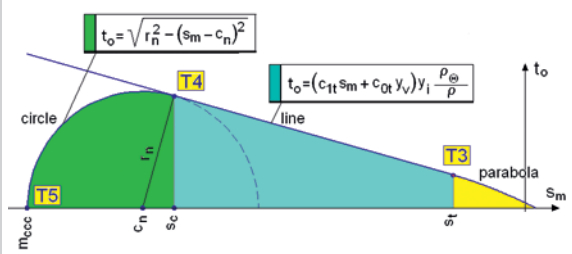

Figure 8.
Construction of the closing cap on the compressive side

The equation of any circular meridian of the cap of the yield surface in the general form looks as follows:

$$t_o(\Theta)=\sqrt{r_n^2-\left(s_m-c_n\right)^2} \quad (36)$$

where:

r_n and c_n are respectively radius and centre of arbitrary circle.

Circles closing yield surfaces from the compressive side must appropriately suit to linear segments. So, radius and centre must be determined with respect to Lode's angle to achieve expectable smoothness. Obviously, to follow change of the yield surface shape during hardening or softening, radius r_n, centre c_n and abscissa s_c of tangential point are also dependent on yield functions values. Considering constraints, that for one yield surface all circles creating its cap must intersect in one point on the mean stress axis, all of them must be tangentially joint with linear parts of meridians, and abscissa s_c should fulfil condition $s_c < s_t$, following formulas have been obtained for:

radius:

$$r_n=\frac{\rho_\Theta y_i\left(\sqrt{c_{1t}^2y_i^2\rho_\Theta^2+\rho^2}+c_{1t}y_i\rho_\Theta\right)\left(c_{1t}m_{ccc}y_{vc}+c_{0t}y_v\right)}{\rho^2} \quad (37)$$

abscissa of the centre point:

$$c_n=m_{ccc}y_{vc}+r_n \quad (38)$$

abscissa of the tangential point:

$$s_c=\frac{\rho^2\left(m_{ccc}y_{vc}+r_n\right)-c_{1t}c_{0t}\rho_\Theta^2y_i^2y_v}{c_{1t}^2y_i^2\rho_\Theta^2+\rho^2} \quad (39)$$

In the above mentioned formulas another yield function y_{vc} is used. This function guides the evolution of the compressive cap. Values of this function depends on the plastic volumetric strains. Negative volumetric strain results in material hardening and in consequence leads to expansion of the cap towards hydrostatic compression, while the dilatation results in softening and causes shrinking of the cap towards beginning of the coordinate system. This cap never shrinks in the softening process as the stress-paths influencing here never generate the dilatation.

5. CONCLUSIONS

There are many examples of reinforced concrete members, that thanks to introducing elasto-plastic material model for concrete can be analysed more precisely. Although, much more sophisticated models exist, such a simple description of concrete can suit in macro scale analysis. Description of material behaviour is always composition of results obtained in laboratory conditions and theoretical prediction. Because, material model cannot be fully formed on experiments, so there is also a space for logical assumptions. Equations presented above was derived to approximate results of multi-axial tests and to achieve relatively simple definition of concrete response on the external actions. Computational system *Mafem3D*, where this model is applied was used in several analysis, including: punching shear in RC slabs [18], analysis of spot footings behaviour [19], RC perforated walls analysis [20], as well as simulation of behaviour of samples, used for testing concrete strength properties [21]. Some of these tests results are also presented in [12].

REFERENCES

[1] *Majewski S., Krzywoń R., Wandzik G.*; Numeryczna i doświadczalna weryfikacja pakietu MAFEM do nieliniowej analizy konstrukcji żelbetowej (Numerical and experimental verification of nonlinear FEM system MAFEM used for RC structures analysis). XLV Konferencja Naukowa KILiW PAN i KN PZITB, Vol.2, Wrocław-Krynica, 1999; p. 167-174 (in Polish)

[2] *Majewski S., Wandzik G.*; Two-stage numerical analysis of RC slabs punching capacity. International Workshop on Punching Shear Capacity of RC Slabs, Proceedings, Stockholm, 7-9 June 2000; p.387-396

[3] *Szojda L., Wandzik G.*; Numeryczna analiza zachowania naroży żelbetowych ram portalowych (Numerical analysis of the behaviour of RC portal frame corners). XL Konferencja Naukowa KILiW PAN i KN PZITB, Vol.3, Kraków-Krynica, 1994; p.193-200 (in Polish)

[4] *Majewski S., Krzywoń R., Wandzik G.*; Failure Criteria in Estimation of Load Capacity for Reinforced Concrete Members. Proceedings of the US-Poland Workshop on "Modern Problems of Concrete Structures", Wrocław, 1999; p.43-46

[5] *Szojda L., Wandzik G.*; Homogeniczny, sprężysto-plastyczny model materiałowy do analizy konstrukcji murowych (Homogeneous elasto-plastic material model used for the analysis of masonry structures). Monografia: Problemy naukowo-badawcze budownictwa. Wydawnictwo Politechniki Białostockiej, Vol.2, Konstrukcje budowlane i inżynierskie, Białystok, 2007; p.355-362 (in Polish)

[6] *Krzywoń R., Szojda L., Wandzik G.*; Numerical analysis of building subjected to the ground subsidence. 6th International Scientific Conference „Analytical Models and New Concepts in Concrete and Masonry Structures", Łódź, 2008; p.331-332, full version published on CD

[7] *Willam K. J., Warnke E. P.*; Constitutive Models for the Triaxial Behaviour of Concrete. Int. Ass. of Bridge Struct. Eng. Proc. Vol.19, 1975; p.1-30

[8] *Balmer G.G.*; Shearing Strength of Concrete under High Triaxial Stress Computation of Mohr's Envelope Curve. Bur. Reclam. Struct. Res. Lab. Rep. SP23, 1949

[9] *Kupfer H., Hilsdorf K., Rusch H.*; Behaviour of Concrete under Biaxial Stresses. Journal of American Concrete Institute, Vol.66, No.8, 1969; p.656-666

[10] *Richart F. E., Brandtzaeg A., Brown R. L.*; A Study of the Failure of Concrete under Combined Compressive Stresses. Univ. Ill. Eng. Exp. Stn. Bull, 1928, 185 Urbana

[11] *Mills L.L., Zimmerman R.M.*; Compressive Strength of Plain Concrete under Multiaxial Loading Conditions. Journal of American Concrete Institute, Vol.67, No.10, October, 1970; p.802-807

[12] *Majewski S.*; Mechanika betonu konstrukcyjnego w ujęciu sprężysto-plastycznym (Mechanics of structural concrete in elasto-plastic formulation). Monografia, Gliwice, 2003 (in Polish)

[13] *Ottosen N. S.*; A Failure Criterion for Concrete. J. Eng. Mech. Div. ASCE, Vol.103, 1977; p.527-535

[14] *Oluokun F.A.*; Prediction of Concrete Tensile Strength from Compressive Strength. Evaluation of Existing Relations for Normal Weight Concrete. ACI Materials Journal, Vol.88, No.3, 1991; p.302-309

[15] Podstawy projektowania konstrukcji żelbetowych i sprężonych według Eurokodu 2 (Basis of reinforced concrete and prestressed concrete structures design according to Eurocode 2). Dolnośląskie Wydawnictwo Edukacyjne, Wrocław, 2006; 976p (in Polish)

[16] EN-1992-1-1 (Eurocode 2):2004; Design of concrete structures. Part 1-1: General rules and rules for buildings. CEN, Brussels, December 2004; 230p

[17] *Flaga K.*; Wpływ rodzaju kruszywa na kruchość betonów wysokich marek (Influence of the aggregate type on the brittleness of high strength concrete). Inżynieria i Budownictwo, No.2, 1974 (in Polish)

[18] *Wandzik G., Majewski S.*; Analysis of 3D Stress-State in RC Slab-Column Connection. 2nd European Conference on Computational Mechanics (Solids, Structures and Coupled Problems in Engineering), abstracts, Vol.2, Kraków, 2001; p.1098-1099 (full version published in electronic version)

[19] *Majewski S., Wandzik G.*; Analiza zachowania żelbetowej stopy fundamentowej (Analysis of the RC spot footing behaviour). Zeszyty Naukowe Politechniki Śląskiej, No 1288, Seria: Budownictwo, Vol.80, 1995; p.53-64 (in Polish)

[20] *Jóźwiak I., Wandzik G.*; Badania laboratoryjne i numeryczne gęsto perforowanych ścian betonowych poddanych jednoczesnemu ścinaniu i zginaniu (Experimental and numerical tests performed for densely perforated concrete walls subjected to simultaneous shear and flexure). XLIV Konferencja Naukowa KILiW PAN i KN PZITB, Vol.4, Poznań-Krynica, 1998; p.77-85 (in Polish)

[21] *Ajdukiewicz A., Majewski S., Kliszczewicz A., Wandzik G.*; Numerical and Experimental Analysis of Models used for Testing of Compressive Strength. II International Scientific Conference „Analytical Models and New Concepts in Mechanics of Concrete Structures", Łódź, 1996; p.31-36